Reactor test of beryllium as self-powered neutron detector emitter for fast neutron flux measurement

Elsa Dupin[1], Loïc Barbot[1,*], Stéphane Normand[2], Jean-Marc Fontbonne[3], Nicolas Thiollay[1] and Christophe Destouches[1]
[1]CEA, DES, IRESNE, DER, Cadarache, F-13108 Saint Paul-lez-Durance, France
[2]CEA DAM Île-de-France Bruyères-le-Châtel, 91297 Arpajon cedex, France
[3]Laboratoire de Physique Corpusculaire, ENSICAEN, 6 Bd Maréchal Juin, 14000 Caen, France
(*) corresponding author loic.barbot@cea.fr

***Abstract*— Neutron flux in nuclear reactors causes damages to material components. Fast neutrons, above 1 MeV, modify mechanical and structural properties of materials. Some experiments carried out in research reactors study the ageing of materials exposed to high neutron fluxes. In these experiments, the selective on-line monitoring of fast neutron flux in a water-pool type reactor environment remains a measurement challenge. The aim of this work is to experimentally validate the use self-powered neutron detector technology to monitor fast neutron flux in a water-cooled reactor.**

After a systematic review of the periodic element table, beryllium appears to be the most suitable emitter material for measurements sensitive and selective to fast neutrons. Due to its threshold cross section to neutrons and its low interaction probability with gamma rays, beryllium seems the appropriate candidate as emitter material for reactor environment use. Beryllium SPND prototypes were designed and manufactured.

In June 2024, beryllium SPND prototypes have been tested in the Slovenian TRIGA Mark II reactor (Jožef Stefan Institute - JSI). These specific reactor tests in well-characterized irradiation conditions could enforce fast neutron SPNDs as a new option for on-line monitoring of technological irradiations.

***Keywords* — Self-powered neutron detector, SPND, fast neutron, neutron flux measurement.**

I. Introduction

In material testing reactors (MTR), like future Jules Horowitz Reactor (JHR), accelerated ageing of nuclear reactor components is achieved through high neutron flux exposition as anticipation of structural changes and potential embrittlement, fast neutrons being the main cause of steel damages during mixed neutron and gamma irradiations due to atom displacements. Currently, on-line measurement of fast neutrons flux in a water pool-type reactor environment remains a challenge to monitor long-term irradiation experiments. The CEA Fast Neutron Detection System (FNDS) [1], composed of two fissions chambers coupled with an evolution code is the one of the very few existing system for on-line monitoring of fast neutron fluxes in research reactors.

Self-Powered Detectors (SPDs) have been developed since the 1960s for on-line measurement of thermal neutron flux [2-4], and recently for γ ray flux measurement [5]. This work falls in the frame of an attempt to drive the SPD technology toward a fast neutron selective self-powered neutron detector (SPND).

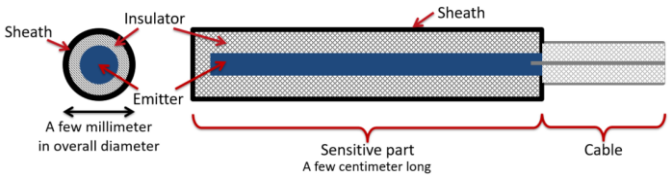

Fig. 1. Standard Self-Powered Detector scheme.

SPNDs are coaxial detectors that operate without high voltage, generally composed of three components: an emitter, an insulator and a sheath. Operating only for high fluxes, SPNDs are ideally adapted to on-line monitoring of irradiation experiments. Material choice and, in particular, emitter choice favor interactions with specific particles of interest. In our case, SPND material design must maximize fast neutron contribution.

A preliminary phase consisted of designing a detector mostly sensitive to fast neutrons in an environment where thermal neutrons and γ rays are predominant [6]. Using an in-house SPND simulation tool [7] and on purpose advanced model based on the Shockley-Ramo theorem [8], a SPND design was developed with high enough confidence meriting prototype fabrication and the set-up of a dedicated experimental campaign in the JSI TRIGA Marl II reactor.

Tests first qualified the irradiation locations with different measurements techniques such as dosimetry, standard SPD measurements and axial profiles with fission chambers and ionization chamber. It also validates the irradiation conditions (thermal neutrons, fast neutrons, and gamma rays) in support of dedicated TRIPOLI4® [9] calculations for each experimental location.

Then, the study focuses on performance analysis of the beryllium SPND prototypes in a reactor environment. The analysis yields encouraging outcomes, particularly following a

© The Authors, published by EDP Sciences. This is an open access article distributed under the terms of the Creative Commons Attribution License 4.0 (https://creativecommons.org/licenses/by/4.0/).

comparison with SPND numerical modelling. These results permit an evaluation of beryllium benefits as an emitter.

II. Design and Fabrication of Fast Neutron Sensitive Prototypes

A. *Emitter material identification*

Fig. 2 presents in lethargy unit neutron and γ spectra in the Slovenian TRIGA Mark II reactor MP17 experimental location, used to design a SPND sensitive to neutrons with an energy above 1 MeV. In this location, both total neutron flux level γ-ray flux level are roughly $2 \cdot 10^{13}$ p·cm^{-2}·s^{-1} (particles integrated over the respective whole energy spectrum).

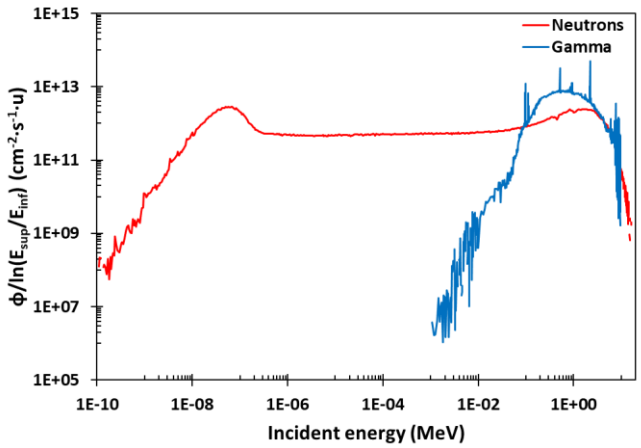

Fig. 2. Energy spectra in lethargy unit, in Slovenian TRIGA Mark II reactor MP17 position (calculated), with a neutron and γ ray total flux level of ~$2 \cdot 10^{13}$ cm^{-2}·s^{-1} each.

Main constraint is thermal neutron presence, whose capture cross-sections are generally much larger than fast neutron ones. The (n, γ) reaction is usually the major one in a standard SPNDs. Cross-sections are generally of up to several hundred barns for neutrons with an energy below 0.625 eV (thermal neutrons), whilst only a few 0.1 barn at most for neutrons with an energy around 1 MeV (fast neutrons). γ rays from the reactor environment may also create a significant additional contribution to the SPND current.

The few main criteria for a good emitter material candidate are metallic shape (good charge conductivity) and generator of a β$^-$ emitter with a relatively short half-life and a sufficient enough energy to leave the emitter and reach the insulator. At the end, materials and associated dimensions have to integrate these constraints while making the SPND output signal mainly representative to the fast neutron flux level.

Based on a systematic review of the periodic element table [6], the most promising material as SPND emitter is beryllium, only composed of one isotope: ^{9}Be. It is also confirmed by a literature survey [10-12], but applications were for fusion or fast reactor. Beryllium, with its (n, α) threshold interaction (667 keV) is creating ^{6}He, emitting 1.6 MeV β$^-$ particles with 808 ms half-life [13]. No other neutron interactions generate any charge significant to the SPND signal. This is confirmed on Fig. 3 which presents the convoluted neutron reaction rate on beryllium in the TRIGA Mark II reactor, calculated with equation (1).

$$R_n(E_n) = N_{mat} . \sigma(E_n) . \phi(E_n) \quad (1)$$

Where $R_n(E_n)$ is the neutron reaction rate at neutron energy E_n [cm^{-3}·s^{-1}];
N_{mat} is the bulk density of studied isotope [cm^{-3}];
$\sigma(E_n)$ is the cross-section at E_n [cm^2];
$\phi(E_n)$ is the neutron flux at E_n [cm^{-2}·s^{-1}].

Using cross-sections from ENDF/B-VIII library [14], reaction rates are calculated for interactions that produce radioactive β isotopes with short enough half-lives. Fig. 3 confirms the absence of any neutron interaction in the thermal and epithermal energy range below 667 keV.

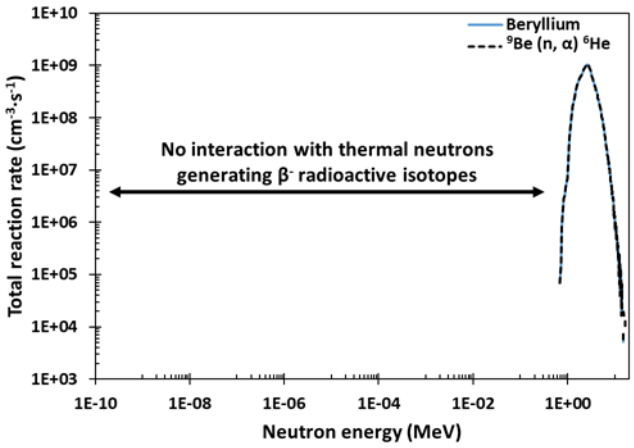

Fig. 3. Neutron reaction rate on beryllium, calculated using TRIGA Mark II neutron spectrum. No neutron interaction in the thermal and epithermal energy range.

Literature does not mention any reactor tests with a Be emitter SPND. However, Raj [11] presented and tested this emitter under a 14 MeV neutron generator. Beryllium is believed to be an interesting emitter material for water pool-type reactor application providing an optimized design.

B. *SPND prototype design*

To validate this innovative material emitter, the other SPND components (insulator and sheath) are chosen from materials commonly used in SPND fabrication: Inconel600® sheath and magnesia insulator for their respective low cross-sections to thermal neutrons

Starting from the CEA MATiSSe simulation tool [7, 15], an advanced model based on the Shockley-Ramo theorem [16, 17] was developed to deal with low sensitivity SPND case where multiple weak contributions are competing against each other and giving rise to a non-monotonous electric field in the insulator [8]. This was used for a parametric study of the beryllium emitter geometry to determine an optimum beryllium rod diameter.

Fig. 4 presents parametric results of the total SPND current to expect and its main contributions for the emitter diameter variation from 2 to 6.5 mm. Configuration with a ∅4 mm beryllium emitter is found to be the most relevant as thermal neutron and gamma contributions tend to cancel each other out,

resulting a total current of almost 3.8 nA (20 cm long emitter), supposedly due at 93.4% to fast neutrons.

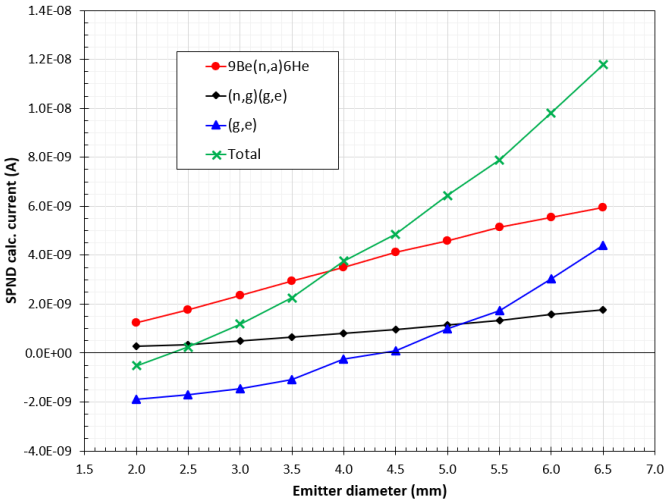

Fig. 4. Beryllium emitter SPND total current and main contributions calculated for different emitter diameter values from 2 to 6.5 mm.

In conclusion to the design phase, beryllium SPND prototypes were proposed with the global geometry presented on Fig. 35, including a ∅4 mm beryllium emitter, a 0.9 mm thick MgO insulator and a 0.2 mm thick Inconel600® sheath, making a ∅6.6 mm overall diameter detector.

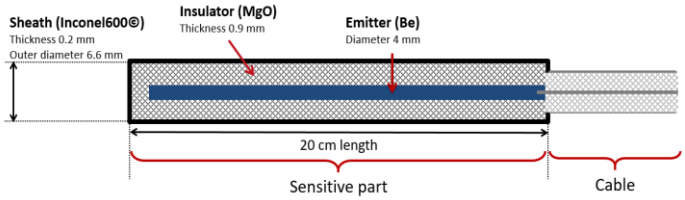

Fig. 5. Beryllium SPND design with a ∅4 mm and overall diameter of 6.6mm.

C. *Be SPND prototype fabrication*

Beryllium was identified as the best option for a fast neutron selective SPND, nevertheless it's a material with many constraints when it comes to processing. Considered as double use good with regards to nuclear non-proliferation regulations, even raw material requires export control license and end-user certificate. Being also carcinogenic material, machining and handling requires precautions and glove box use.

Five Be SPND prototypes were finally assembled by the Photonis – Exosens Group company (Brive-la-gaillarde, France) using ∅1 mm Inconel600® MI cable from the Thermocoax company (Caligny, France).

Three Be SPND prototypes were tested in the JSI TIGA Mark II reactor.

III. Reactor Tests

Be SPND prototypes were irradiated through incore reactor tests during a dedicated CEA experimental campaign, along with side neutron and gamma monitors for irradiation location thorough characterization.

A. *Experimental Location Characterization*

Three incore experimental locations (A1, C3 and F6) were picked within the TRIGA Mark II reactor core for the tests (see Fig. 6). They present identical geometry (Ø34.5mm aluminum tubes) but rather different neutron and gamma flux levels and spectra. Those were assessed using a combination of activation foils, U235 and U238 CEA miniature fission chambers, miniature ion chamber and CEA unfolding method.

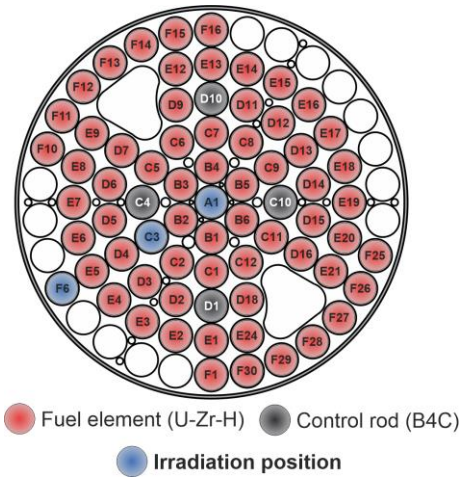

Fig. 6. Sketch of the TRIGA Mark II top view, including fuel elements (red), control rods (grey) and experimental locations (blue).

Absolute neutron (including three energy bins) and gamma flux levels along with neutron and gamma flux profiles were then achieved in the three experimental locations. All data are presented on Fig. 7 to 9 and Table I. Axial profiles ware also performed to get integrated neutron and gamma flux values to be used for Be SPND prototype analysis over their 20 cm emitter length.

Delayed gamma flux proportion to the total gamma flux was experimentally estimated using the reactor SCRAM (*Safety Control Axe Man*) operation mode.

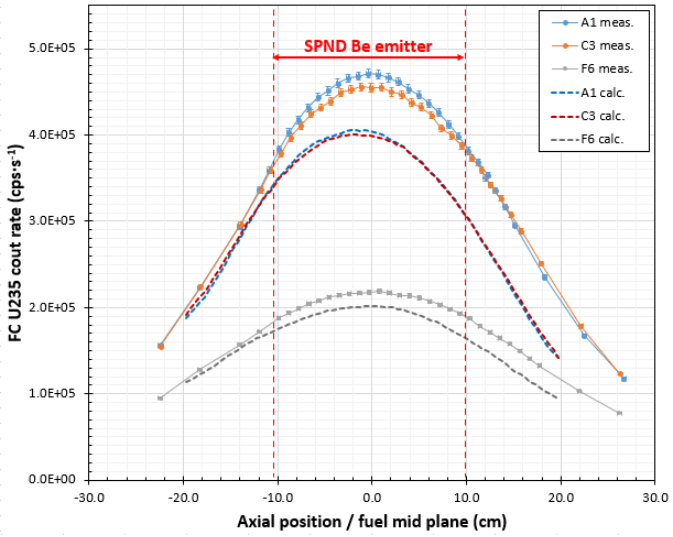

Fig. 7. U235 miniature fission chamber axial profiles in A1, C3 and F8 experimental locations (experiment to calculation comparison).

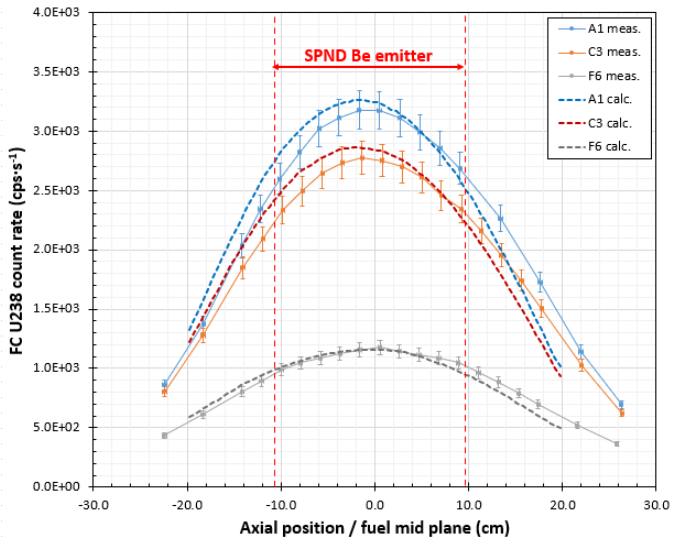

Fig. 8. U238 miniature fission chamber axial profiles in A1, C3 and F8 experimental locations (experiment to calculation comparison).

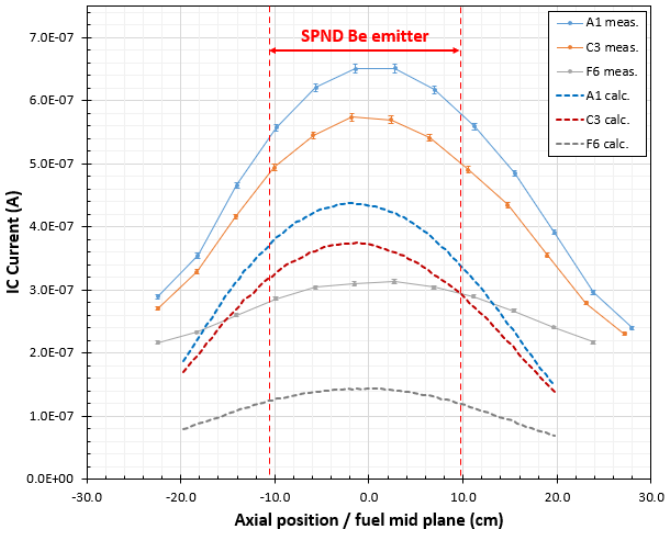

Fig. 9. Miniature ion chamber axial profiles in A1, C3 and F6 experimental locations (experiment to calculation comparison).

TABLE I. NORMALIZED NEUTRON AND GAMMA FLUXES IN THE A1, C3 AND F6 EXPERIMENTAL LOCATIONS OF THE TRIGA MARK II REACTOR

Exp. location	**A1**	**C3**	**F6**	
Power		250kW		
$\phi_{n,\text{total norm.}}$	$2.25\cdot10^{13}$	$1.95\cdot10^{13}$	$7.62\cdot10^{12}$	($n.cm^{-2}.s^{-1}$)
$\phi_{<0.630eV}$	37.4%	42.5%	55.0%	
$\phi_{0.630eV<E<1MeV}$	25.9%	24.7%	20.1%	
$\phi_{>1MeV}$	36.7%	32.8%	24.9%	
$\phi_{\gamma,\text{total norm.}}$	$4.27\cdot10^{13}$	$3.70\cdot10^{13}$	$1.40\cdot10^{13}$	($\gamma.cm^{-2}.s^{-1}$)
$\%\phi_{\gamma,\text{delayed}}$	41.9%	40.4%	41.6%	

B. *Standard SPD Tests*

Along with the three Be SPND prototypes, some CEA standard SPDs were also tested in the A1, C3 and F6 experimental locations to confirm the neutron and gamma data consistency using CEA models and tools for SPND simulations [6, 8]. Standard SPDs, including rhodium, cobalt and tubular bismuth (SPGD) emitters, full geometries are presented on Fig. 10.

Measured and calculated currents are compared in Table II with C/E (calculation to experiment) ratios consistent with previous results [15]

TABLE II. STANDARD SPD C/E COMPARISONS IN THE TRIGA MARK II REACTOR

SPND	**Rhodium**	**Cobalt**	**Bismuth**	
Location		A1		
$I_{measured}$	38.8±0.1	6.45±0.06	10.7±0.4	(nA)
$I_{calculated}$	35.3*	5.30*	12.6*	(nA)
C/E	0.91	0.82	1.18	

* *Statistical uncertainties < 1%*

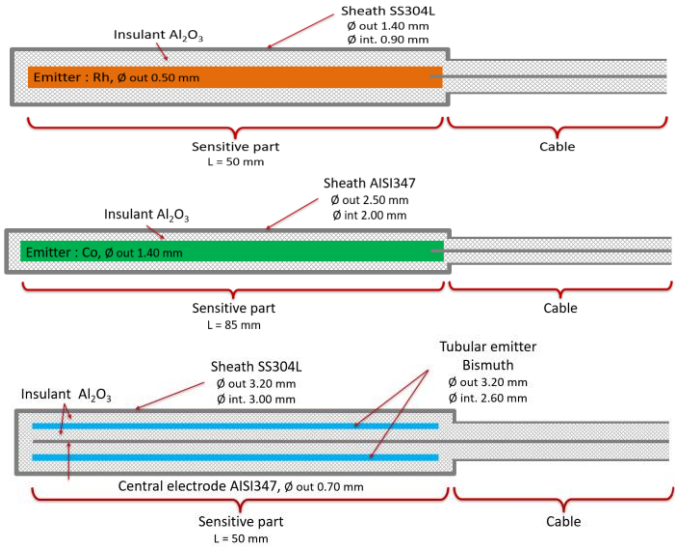

Fig. 10. Geometries of standard CEA SPNDs (rhodium, cobalt and bismuth emitters respectively)

C. *Beryllium SPND Prototype Tests*

The three Be SPND prototypes are each mounted in individual irradiation rigs (Fig. 11) made out of an aluminum tube. It is equipped with a large clearance to limit neutron and gamma attenuation, and some winglets at 120° for a precise and reproducible axial positioning in the center of experimental locations. The irradiation rig height is designed to lay SPND emitters at the fuel mid plane.

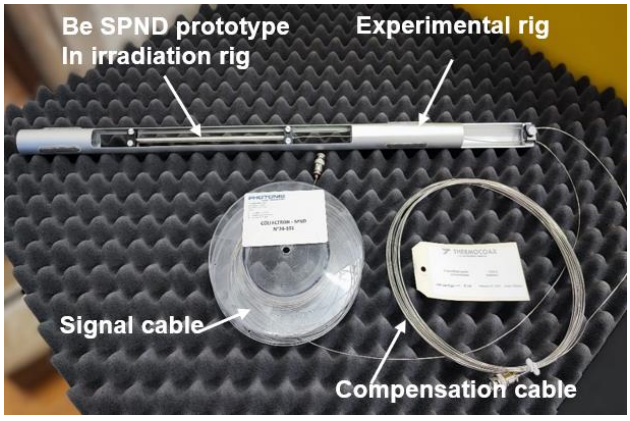

Fig. 11. Beryllium SPND irradiation rig

Fig. 11 also shows a compensation cable used along with one of the prototypes and stopping before the sensitive part to enable a posteriori cable current correction.

The three Be SNPD prototypes were irradiated and shuffled within the three irradiation locations several times to test their reproducibility as well as their sensitivities to the three different mixed fields. The TRIGA Mark II reactor was operated on purpose at different power steps to check prototype linearity and during different transient operations (ramp-up, SCRAM, cooling…) to address the prototype behavior and time response.

As example, Fig. 12 shows the three prototype currents over time during three reactor power steps (50, 150 and 250 kW).

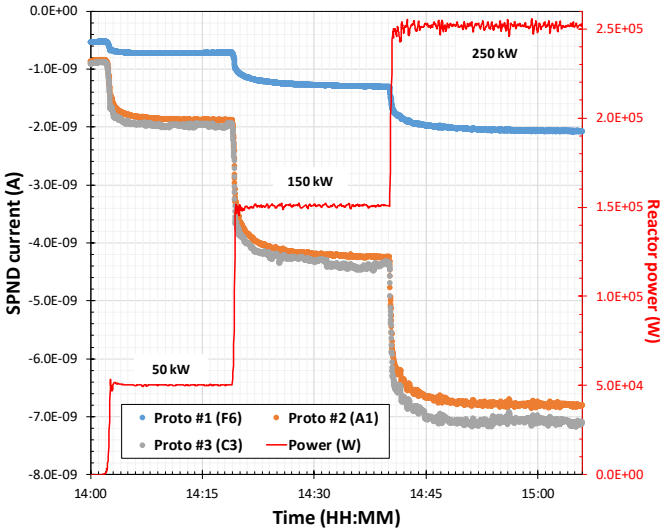

Fig. 12. Beryllium SPND prototype currents during reactor power steps.

For the two central core locations, Be SPND currents stabilized around a negative value of -7nA, to be compared to the ~4 nA expected value (see section II.B).

The rest of this document will focus on explaining what went wrong although it is still demonstrating the value of beryllium for a fast neutron sensitive SPND.

IV. Unexpected Result Analysis

A. *False representativeness of sizing data*

The complete design phase of the Be emitter SPND was achieved using commonly used neutron and gamma data coming from numerous past (mostly thermal neutron oriented) experiments in rather close incore irradiation locations in the TRIGA Mark II reactor, which was never an issue while designing new experiments/detectors.

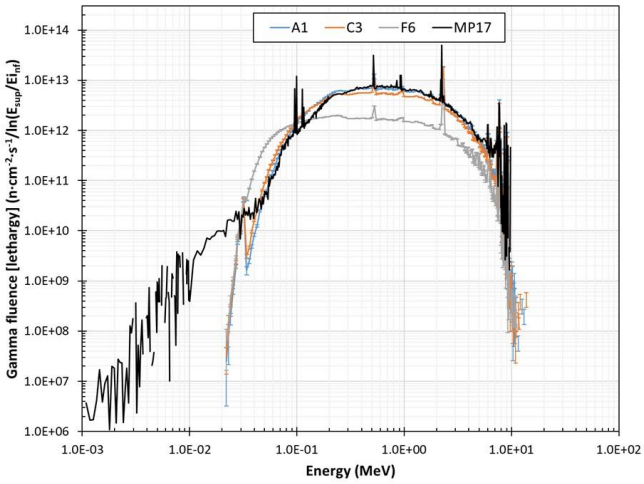

Fig. 13. Comparison of sizing gamma spectrum in MP17 to experiment gamma spectra (all calculated).

Unfortunately, attention was not paid enough to the gamma contribution and therefore to the gamma flux level and spectra definition. Up top now, gamma contribution to SPNDs was not in competition with the neutron one, it was addressed only for accuracy purposes. Here, the design phase demonstrated almost balanced fast neutrons and gamma contributions.

Fig. 13 shows differences between sizing gamma spectrum and actual gamma spectra determined during the tests, that probably explain the unexpected stronger and negative values of the prototype currents.

B. *Use of transient operation data recordings*

Thorough analysis of Be SPND recordings during SCRAM transients highlights a recurrent behavior of SPND currents always few seconds after reactor shut downs.

Fig. 14, as example, is showing a negative bump after the current sharp transient due to the SCRAM. Current being negative, the negative bump is due to a decreasing with time positive contribution, which is then progressively counterbalanced by a slowly appearing new contribution.

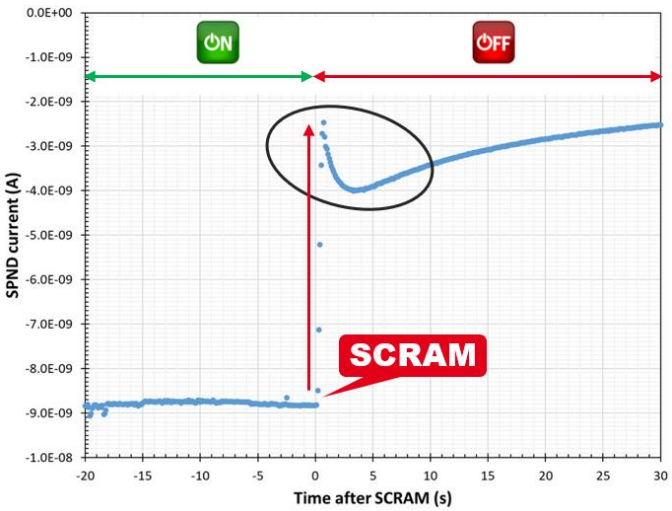

Fig. 14. Beryllium SPND recording after reactor SCRAM.

Studying the superimposition of theoretical contributions to the beryllium SPND, it was found that the observed bump could

reasonably due to the ^{9}Be contribution combined with delayed gamma coming from the reactor core and activated structures, as illustrated on Fig. 15.

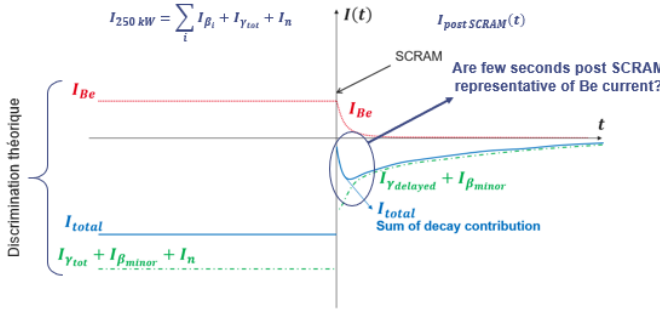

Fig. 15. Theoretical contributions to the beryllium SPND.

Using the Wigner-Way formula [18-20] which describes the decay shape of delayed gamma after a SCRAM, the commented equation on Fig. 16 is developed to model the decay of a Be SPND signal after a SCRAM. It is then possible to dig out the "measured" ^{9}Be currents representative of the fast neutron contribution. Delayed gamma contribution mentioned corresponds to the mean value of delayed gamma percentages experimentally estimated in Section III.A (41.3%).

$$I_{post\,SCRAM}(t) = \sum_{i}^{t=0\,s} I_{\beta_i} \cdot \exp(-\lambda_{\beta_i} \cdot t) + I_{\gamma_{ret}} \cdot (t^{-0,2} - (T_{250kW} + t)^{-0,2}) \qquad \lambda_{\beta_i} = \frac{\ln(2)}{T_{1/2\,\beta_i}}$$

β- contributions

Delayed γ contribution

$$I_{\gamma_{tot}} = \frac{1}{41,3\%} \cdot I_{\gamma_{ret}}$$

Fig. 16. Model developed to describe the decay shape after SCRAM, applied with experimental values. In green, the Wigner-Way formula for γ decay shape [18-20]. In red, contribution currents at t = 0s (SCRAM triggered).

Measured and calculated (using CEA simulation tools) ^{9}Be absolute contributions to the SPND currents are compared for the three experimental locations, showing C/E ratio close to 1 in every location. Moreover, the ^{9}Be contribution value is also close to the 3.8 nA expected in section II.B.

TABLE III
CALCULATED TO MEASURED ^{9}BE CONTRIBUTION COMPARISONS IN DIFFERENT EXPERIMENTAL LOCATIONS. SIGNAL AND FAST NEUTRON RATIOS COMPARISONS

	A1			C3			F6		
	C	E	C/E	C	E	C/E	C	E	C/E
SPND current coming from 9Be (n, α) 6He									
I_{Be} (nA)	3.7	3.2	1.2	2.9	2.8	1.05	0.84	0.79	1.06
Irradiation location ratios									
$\frac{I_{Be_{loc}}}{I_{Be_{A1}}}$	1	1		0.78	0.85		0.23	0.24	
$\frac{\phi_{N_{rap_{loc}}}}{\phi_{N_{rap_{A1}}}}$			1			0.78			0.23

Looking also closely to the ratios between experimental locations in terms of ^{9}Be currents and fast neutron fluxes, they are very consistent among each other.

Gathering all those partial experimental results help the authors to claim that this dedicated experimental campaign validate the use of beryllium as emitter for inline fast neutron flux monitoring.

V. CONCLUSIONS

The initial objective of this work was to design a fast neutron selective SPND in a water reactor environment (high thermal neutrons and γ mixed field). Beryllium SPND prototypes were designed and manufactured including a ^{9}Be emitter, a MgO insulator and an Inconel600® sheath. Qualification tests were conducted at the JSI TRIGA Mark II reactor to evaluate beryllium material suitability.

The proposed design does not give the expected results, with prototype signal mostly sensitive to gamma flux. However, the use of beryllium as SPND emitter is experimentally validated. The signal study at the SCRAM trigger demonstrated the possibility to discriminate different contributions to the total SPND signal and to extract a beryllium contribution which follows the fast neutron flux as expected.

This work thus demonstrates the potential of beryllium as an emitter for online fast neutron measurements, although design optimization work remains to be done to remove the gamma component of the signal.

ACKNOWLEDGMENT

The PhD thesis work of Elsa Dupin was financially supported by the CEA Gen23 program, in the frame of the instrumentation project (INSNU) to develop innovative and advanced nuclear and non-nuclear instrumentation in preparation of the CEA Jules Horowitz Reactor (JHR) commissioning.

REFERENCES

[1] D. Fourmentel, J. F. Villard, C. Destouches, B. Geslot, L. Vermeeren, and M. Schyns, "In-pile qualification of the fast-neutron-detection-system," in *ANIMMA*, Belgium, 2017.

[2] J. W. Hilborn, "Self-Powered Neutron Detectors for Reactor Flux Monitoring," *Instrumentation and Measurements*, vol. 22, no. 2, pp. 69–74, Feb. 1964.

[3] M. Grin, "Collectrons, Self-Powered Neutron Flux Detectors - Part I : Theoretical considerations," Commission of the european communities, EUR4775e, 1972.

[4] O. Strindehag, "Self-Powered Neutron and Gamma Detectors for In-Core Measurements," Studsvik, Nyköping, Sweden, AE-440, Nov. 1971.

[5] H. Carcreff, L. Barbot, and L. Vermeeren, "Gamma radiation detector, and associated method for making same and uses thereof," WO 2010/103049 A1, Sep. 16, 2010

[6] E. Dupin, L. Barbot, S. Normand, JM. Fontbonne, N. Thiollay, "Design and reactor test of a selective fast neutron self-powered detector for applications in water-pool type reactor," Poster presented in 2023 8th International Conference on Advancements in Nuclear Instrumentation Measurement Methods and their Applications (ANIMMA), Lucca, June 2023.

[7] L. Barbot, V. Radulovic, V. Dewynter-Marty, F. Malouch, and F. Lopez, "Experimental validation of a Monte Carlo based toolbox for Self-Powered Neutron and Gamma Detectors simulation in the OSIRIS MTR," presented at the PHYSOR 2016 - Unifying Theory and Experiments in the 21st Century, Sun Valley, Idaho, USA, May 2016.

[8] E. Dupin, L. Barbot, S. Normand, J-M. Fontbonne, N. Thiollay, C. Destouches, "Theory and modelling for the design of a selective fast neutron self-powered detector for applications in water pool type reactors", presented at the 2023 IEEE Nuclear Science Symposium (November 4-11 2023, Vancouver, Canada)

[9] E. Brun, F. Damian, C.M. Diop, E. Dumonteil, F.X. Hugot, C. Jouanne, Y.K. Lee, F. Malvagi, A. Mazzolo, O. Petit, J.C. Trama, T. Visonneau, A. Zoia, Tripoli-4®, CEA, EDF and Areva reference Monte Carlo code, Annals of Nuclear Energy no 82, 2015, p. 151-160

[10] J. W. Jr. Upton, D. P. Brown, and W. G. Spear, "In-core, Self-powered fast neutron flux monitors," presented at the American Nuclear Society Power Division Topical Meeting, Williamsburg, Virginia, Aug. 1970, p. 13. Accessed: Mar. 08, 2022. [Online]. Available: https://www.osti.gov/servlets/purl/4059106

[11] P. Raj, "Development and Testing of Self–Powered Detectors for Nuclear Measurements in Fusion Reactors," PhD Thesis, Department of Mechanical Engineering, Karlsruhe Institute of Technology, 2019. doi: 10.5445/IR/1000096884.

[12] S. Jianxiong *et al.*, "Reactor core fast neutron flux self-powered detector," 2020CN-U3222087, Dec. 28, 2020

[13] Nuclear Energy Agency, "JANIS Web." Accessed: Dec. 17, 2021. [Online]. Available: https://www.oecd-nea.org/janisweb/

[14] D. A. Brown *et al.*, "ENDF/B-VIII.0: The 8th Major Release of the Nuclear Reaction Data Library with CIELO-project Cross Sections, New Standards and Thermal Scattering Data," *Nuclear Data Sheets*, vol. 148, pp. 1–142, Feb. 2018, doi: 10.1016/j.nds.2018.02.001.

[15] L. Barbot *et al.*, "Calculation to experiment comparison of SPND signals in various nuclear reactor environments," in *2015 4th International Conference on Advancements in Nuclear Instrumentation Measurement Methods and their Applications (ANIMMA)*, Lisbon: IEEE, Apr. 2015, pp. 1–7. doi: 10.1109/ANIMMA.2015.7465558.

[16] S. Ramo, "Currents Induced by Electron Motion," *Proc. IRE*, vol. 27, no. 9, pp. 584–585, Sep. 1939, doi: 10.1109/JRPROC.1939.228757.

[23]W. Shockley, "Currents to Conductors Induced by a Moving Point Charge," *Journal of Applied Physics*, vol. 9, no. 10, pp. 635–636, Oct. 1938, doi: 10.1063/1.1710367.

[17] W. Shockley, "Currents to Conductors Induced by a Moving Point Charge," *Journal of Applied Physics*, vol. 9, no. 10, pp. 635–636, Oct. 1938, doi: 10.1063/1.1710367.

[18] T. Van Thuong, O. L. Tashloykov, S. M. Glukhov, D. E. Shumkov, and Yu. V. Volchikhina, Experimental and theoretical justification of passive heat removal system for irradiated fuel assemblies of the nuclear research reactor in a spent fuel pool, Nuclear Engineering and Technology **55**, 2088 (2023).

[19] M. Arkani and M. Gharib, Residual heat estimation by using Cherenkov radiation in Tehran Research Reactor, Nuclear Instruments and Methods in Physics Research Section A: Accelerators, Spectrometers, Detectors and Associated Equipment **596**, 417 (2008).

[20] S. Kadalev, Assessment of residual heat generation at cyclic operation of a research reactor as input data for thermal hydraulic calculations and safety analysis, Annals of Nuclear Energy **72**, 182 (2014).